Biochemical and Biophysical Research Communications 446 (2014) 155–159

Contents lists available at ScienceDirect

Biochemical and Biophysical Research Communications

journal homepage: www.elsevier.com/locate/ybbrc

microRNA-222 modulates liver fibrosis in a murine model of biliary atresia

Wen-jun Shen, Rui Dong, Gong Chen *, Shan Zheng

Department of Pediatric Surgery, Children's Hospital of Fudan University, and Key Laboratory of Neonatal Disease, Ministry of Health, 399 Wan Yuan Road, Shanghai 201102, China

ARTICLE INFO

Article history:
Received 10 February 2014
Available online 22 February 2014

Keywords:
Biliary atresia
microRNA
Liver fibrosis
Murine model

ABSTRACT

microRNA-222 (miR-222) has been shown to initiate the activation of hepatic stellate cells, which plays an important role in the pathogenesis of liver fibrosis. The aim of our study was to evaluate the role of miR-22 in a mouse model of biliary atresia (BA) induced by Rhesus Rotavirus (RRV) infection. New-born Balb/c mice were randomized into control and RRV infected groups. The extrahepatic bile ducts were evaluated. The experimental group was divided into BA group and negative group based on histology. The expression of miR-222, protein phosphatase 2 regulatory subunit B alpha (PPP2R2A), proliferating cell nuclear antigen (PCNA) and phospho-Akt were detected. We found that the experimental group showed signs of cholestasis, retardation and extrahepatic biliary atresia. No abnormalities were found in the control group. In the BA group, miR-222, PCNA and Akt were highly expressed, and PPP2R2A expression was significantly inhibited. Our findings suggest that miR-222 profoundly modulated the process of fibrosis in the murine BA model, which might represent a potential target for improving BA prognosis.

1. Introduction

Biliary atresia (BA) is the leading cause of cholestasis in infants younger than 3 months. The pathology of early BA includes the absence of patent extrahepatic bile ducts (EHBD) with inflammation and fibrosis in the hepatic portal area. Patients with BA suffer from progressive liver fibrosis and cirrhosis, who without treatment, rarely survive over 2 years [1]. Although the Kasai procedure significantly improves the prognosis of BA, most patients still require liver transplantation in their lifetime [2]. The etiology and pathogenesis of BA remains largely unknown. Liver fibrosis is a common clinical manifestation following loss of bile drainage, which contributes to the poor prognosis for BA [3]. Understanding the pathogenesis of liver fibrosis during the progression of BA is critical for the development of therapies.

microRNAs (miRNAs) are endogenous non-coding small (~22 nucleotides) RNA molecules that are able to induce mRNA degradation, inhibit translation and regulate many cellular processes, including cell proliferation, differentiation, apoptosis and embryogenesis [4]. Recent studies indicate that several miRNAs regulate the behavior of inflammatory cells and the deposition of extracellular matrix proteins [5]. Hepatic stellate cells (HSCs) mediate liver fibrosis and have been found to express microRNA-221/222 (miR-221/222) [6]. The upregulation of miR-221/222 was observed in activated HSCs and were indicative of fibrotic progression in animal models [6]. The protein phosphatase 2A subunit B (PPP2R2A) has been shown to be a miR-221/222 target [7]. Protein kinase B (Akt) is a protein serine/threonine kinase that plays a key role in proliferation and migration of HSCs [8]. Full activation of Akt requires the phosphorylation of both Thr-308 and Ser-473 [9]. PPP2R2A is known to negatively regulate Akt activity through the dephosphorylation of Thr-308 of Akt [10].

The roles of PPP2R2A and miR-221/222 in liver fibrosis in a BA model induced by rhesus rotavirus (RRV) have not been explored. Using a computational algorithm, we predicted the PPP2R2A gene (a component of protein phosphatase 2A (PP2A)) as a cellular target of miR-221/222. We validated the association of miR-222 with the PP2A regulatory subunit B α isoform, PPP2R2A, by reporter assays and immunoblots. Hepatic lobule localization of positive immunostaining for pAKT, PCNA, and PPP2R2A was assessed by immunohistochemistry (IHC). Our findings uncover a pathway for the regulation of Akt signaling in BA and provide the basis for considering the potential for miR22 and the Akt pathway as molecular tools that can be used for the diagnosis of patients with BA.

* Corresponding author. Fax: +86 21 64931901.
E-mail address: chengongzlp@hotmail.com (G. Chen).

http://dx.doi.org/10.1016/j.bbrc.2014.02.065
0006-291X/

2. Materials and methods

2.1. Animals

Adult, healthy Balb/c pregnant maternal mice were purchased from SLAC Inc. (Shanghai, China) and isolated in laminar-flow cages. Newborn Balb/c mice were randomized into 2 groups in proportion of 2:1 (experimental group: control group). Pups in the experimental group were inoculated intraperitoneally with 25 μL minimum essential medium (MEM), containing 10^6 pfu of rhesus rotavirus [11]. Control group received 25 μL 2% FCS-MEM. Pups that died due to infection, did not feed or that were cannibalized by their mothers were excluded from further analysis. All mice were weighed every two days and observed for signs of cholestasis (icterus of the non-fur-covered skin, color and quality of stools, and the appearance of bilirubin in the urine) until 14 days when they were euthanized. Each liver section was isolated, fixed in formalin and imbedded in paraffin. Each block of paraffin was cut into approximately 10 sections along the hepatoduodenal ligament. All sections were stained with hematoxylin and eosin (H&E). Liver tissues for PCR and western blot were stored at −80 °C. The Ethics Committee at the Children's Hospital of Fudan University approved all studies.

2.2. RNA extraction and quantitative real-time RT-PCR (qRT-PCR)

Total RNA was isolated from liver tissues using Trizol reagent (Ambion, USA) and 5 μg was reverse transcribed using the fist strand RT kit (Thermo Scientific, Boston, USA). mRNA levels were quantified by QuantiTect. SYBR Green reverse-transcription polymerase chain reaction (RT-PCR) kit (TaKaRa Biotech Co., Dalin, China) was used according to the manufacturer's protocol. Quantitative real-time RT-PCR (qRT-PCR) was performed using an ABI 7500 instrument (Applied Biosystems 7500, ABI, Foster City, CA, USA). Serial dilutions of sample RNA were also included to generate a standard curve that was used to calculate the relative concentrations of transcripts in each RNA sample. The sequences were as follows: (1) PPP2R2A: 5′-CATACCAGGTGCATGAATACCTC-3′ (forward) and 5′-GGTTATGTC TCGCTTTGTGTTT-3′ (reverse); (2) PCNA: 5′-TTGCACGTATATGCCG AGACC-3′ (forward) and 5′-GGTGAACAGGCTCATTCATCTCT-3′ (reverse); and (3) GAPDH: 5′-ATGACATCAAGAAGGTGGTG-3′ (forward) and 5′-CATACCAGGAAATGAGCTTG-3′ (reverse). The *GAPDH* housekeeping gene was used for normalization. All PCR reactions were performed in triplicate.

2.3. Protein isolation and Western blot analysis

Three samples were randomly picked from each group. Frozen tissue samples (20–90 mg) were homogenized in 200–900 μL of ice-cold RIPA buffer (Beyotime, P0013C, China). After a 30 min incubation on ice, samples were centrifuged at 21475 g for 5 min at 4 °C and supernatants were collected. Protein concentrations were determined by BCA kit (Beyotime, P0009, China). Protein samples were electrophoresed on 10% denaturing sodium dodecyl sulfate polyacrylamide gels and transferred to a polyvinylidene difluoride (PVDF) membrane. The membrane was incubated with primary antibodies (rabbit anti-mouse, Proliferating cell nuclear antigen, PCNA; rabbit anti-mouse, PPP2R2A; rabbit anti-mouse, p-Akt; rabbit anti-mouse, Akt, (Abcam, UK) 1:1000 in 5% (w/v) non-fat dry milk overnight. After three 5 min washes with Tris-Buffered Saline with Tween 20 (TBST), membranes were further incubated with goat anti-rabbit IgG secondary antibodies conjugated to horseradish peroxidase (Santa Cruz, USA) (1:1000) for one hour at room temperature. Following washing with TBST, membranes were visualized with chemiluminescent substrate (Immobilon Western HRP, Millipore) and imaged using a fusion imaging system.

2.4. Immunohistochemistry

The liver sections were first deparaffinized with xylene and hydrated with 95% ethanol solution. After antigen heat retrieval in citrate buffer (pH 6.0) for 10 min, the sections were allowed cool to room temperature and then washed twice for 2 min in phosphate buffered saline (PBS). Sections were incubated with primary antibodies (1:100) for 2 h at room temperature. Next, the membranes were washed twice for 2 min in PBS and stained with 3,3′-diaminobenzidine tetrahyochloride (DAB). The sections were counterstained with hematoxylin. After washing again twice with PBS, the sections were dehydrated, cleared and mounted. The slides were viewed by Olympus microscope and Medical image analysis software was used to determine the positive areas of PPP2R2A staining and the image intensity. The intensity class index was defined as positive area × image intensity. Cell nuclei with brown granules were positive for PCNA. Percentage of positive cells was calculated for every slice.

2.5. Statistical analysis

Data were expressed as the mean ± standard error of the mean (SEM). The Student's *t*-test was used to determine statistically significant differences between groups. p-values <0.05 were considered statistically significant. All analyses were performed using the SPSS Version 13.0 software.

3. Results

3.1. Clinical manifestation

The control group consisted of 15 mice with one mouse being excluded from analysis due to premature death. Thirty newborn mice received RRV infection intraperitoneally, and 4 mice died either due to infection, not feeding or cannibalized by their mothers. The experimental group consisted of 26 pups. Fourteen (53.8%) mice showed signs of cholestasis (Fig. 1A). Furthermore, the experimental group was characterized by growth retardation (Fig. 1B).

3.2. Histomorphological evaluation

All mice were euthanized on day 14 and autopsies were conducted. The 14 mice in the experimental group had occluded extrahepatic bile lumens with atrophy and fatty deposits in the liver parenchyma, and these mice were classified as the BA group (Fig. 2B). The remaining 12 mice in the experimental group were classified as the negative group (Fig. 2C). No abnormalities were observed in the control group (Fig. 2A). The extrahepatic bile ducts (EHBDs) of mice in the BA group were replaced by fibrotic framework. Sections revealed atresia with either total or interrupted EHBD occlusion in the BA group (Fig. 2B), while the EHBD lumens were patent in both the control (Fig. 2A) and negative groups (Fig. 2C). Histologically, a severe diffuse proliferation of intrahepatic bile ducts (IHBDs) with focal necrosis in the lobuli could be detected in both the BA group and the negative group (Fig. 2D). The negative group had patent IHBD (Fig. 2F), and which were occluded in the BA group (Fig. 2E). The IHBD walls showed edematous swelling with and contained leucocytes within (Fig. 2E).

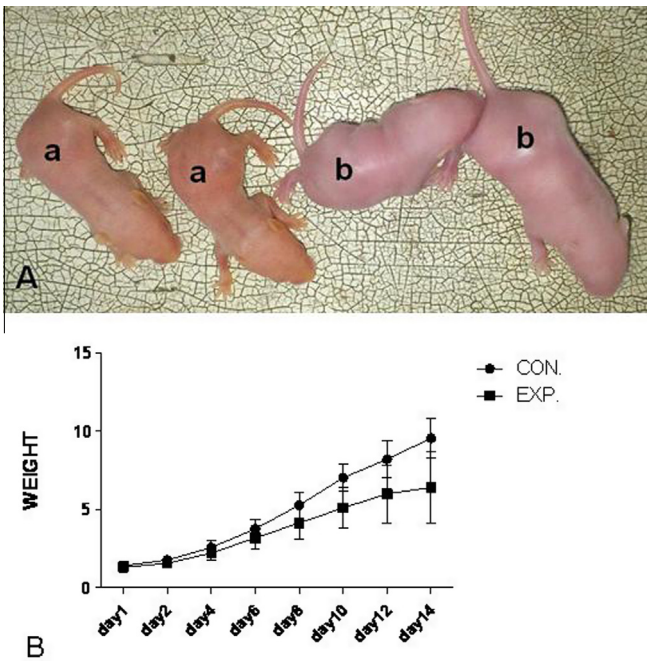

Fig. 1. (A) Pups in the experimental group (a) were wasting and icteritious compared with those in the control group (b). (B) Weight curves showed marked growth retardation in the experimental group during the first fourteen days after birth.

3.3. Effects of microRNA on mRNA expression levels

Expression of miRNA and mRNA in the three groups was evaluated. We found a significantly higher expression level of miR-222 in the BA group (1.99 ± 0.88, $p < 0.05$), while the negative group's value close to the control group (0.98 ± 0.25 *vs.* 1.11 ± 0.28, $p > 0.05$). In contrast, PPP2R2A expression was decreased in the BA group compared with the other two groups (0.63 ± 0.43, $p < 0.05$), while the negative group was lower than the control group (0.81 ± 0.37 vs. 1.12 ± 0.36, $p < 0.05$). PCNA expression was elevated in the BA group (1.93 ± 0.96, $p < 0.05$), and the negative group had the lowest levels of PCNA (0.87 ± 0.22 *vs.* 1.22 ± 0.48, $p < 0.05$).

3.4. Effects of microRNA on protein synthesis

Western blot analysis showed marked differences in protein expression among the three groups (Fig. 3). When the BA group was compared with the control group, there was decreased PPP2R2A and increased PCNA and p-Akt ($p < 0.05$). When the BA group was compared with the negative group, there was decreased PPP2R2A levels and upregulation of p-Akt ($p < 0.05$). The endogenous control GAPDH was stable among the three groups.

3.5. Expression levels of PPP2R2A and PCNA in liver tissue specimens

We then analyzed PPP2R2A and PCNA expression in the liver sections (Fig. 4). PPP2R2A positive staining was detected in the cytoplasm with brown staining in the liver sections. Intensity class index of the control group was 23.93 ± 10.83, while the index for the BA and the negative groups were 6.57 ± 1.65 and 9.73 ± 2.85, respectively. The control group had a higher index ($p < 0.05$), while the other two groups showed no difference. Higher cell proliferation with increased PCNA staining was observed in the BA group (15.32 ± 2.42), while the percentage staining in the control and negative groups were 7.66 ± 1.66 and 8.88 ± 2.94. The BA group had a higher percentage of PCNA positive staining ($p < 0.05$), while the other two groups showed no difference.

4. Discussion

In our study, we successfully utilized a BA murine model based on methods first reported by Petersen [11]. The rate of BA in the experimental group was 53.8%. This was relatively low due to the exclusion of 6 pups that died prematurely following infection. Histopathological changes in the BA group were consistent with previous reports characterized by the ballooning of hepatocytes and presence of giant cells, cellular and canalicular cholestasis, portal tract infiltration, ductular proliferation, lobular necrosis and fibrosis [11]. The negative group was characterized by mild inflammation with patent bile ducts.

Recent studies have demonstrated that miR-29, miR-199 and miR-200 families have important roles in the pathogenesis of liver fibrosis [12,13]. HSCs and hepatic fibrosis have been demonstrated to be associated with elevated miR-221/222 levels. miR-221/222 was upregulated in the liver in a fibrosis progression-dependent

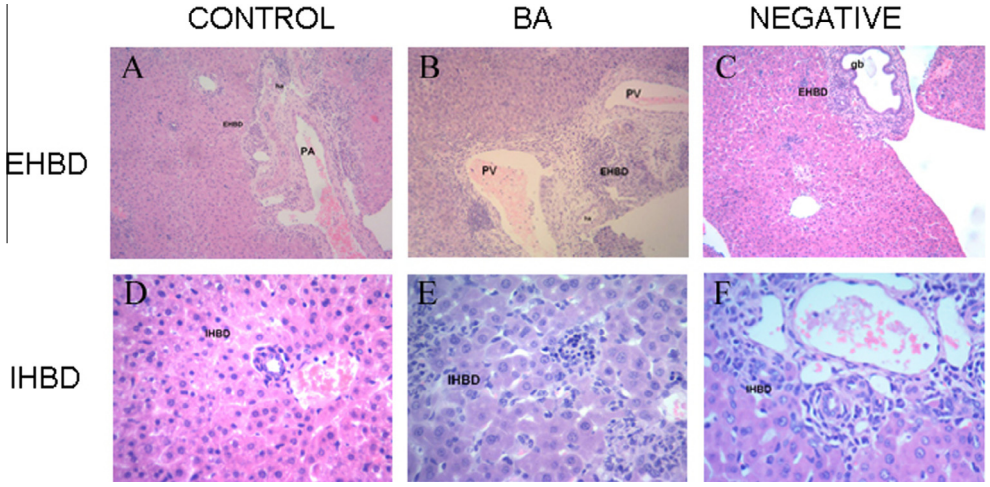

Fig. 2. (A–C) Histological section of the hepatic portal: ha, hepatic artery; PV portal vein; gb, gall bladder (H&E, original magnification × 100). EHBD in the BA group (B) shows EHBD occlusion due to biliary proliferation and fibro deposition. EHBD lumens can be observed in both the control group (A) and the negative group (C). (D–F) IHBD are shown in these sections (H&E, original magnification × 400). The IHBD wall shows biliary proliferation and edematous swelling with leucocytes in both the BA group (E) and the negative group (F) when compared with the control group (D). The negative group maintained patency of IHBD (F), while IHBD was occluded in the BA group (E).

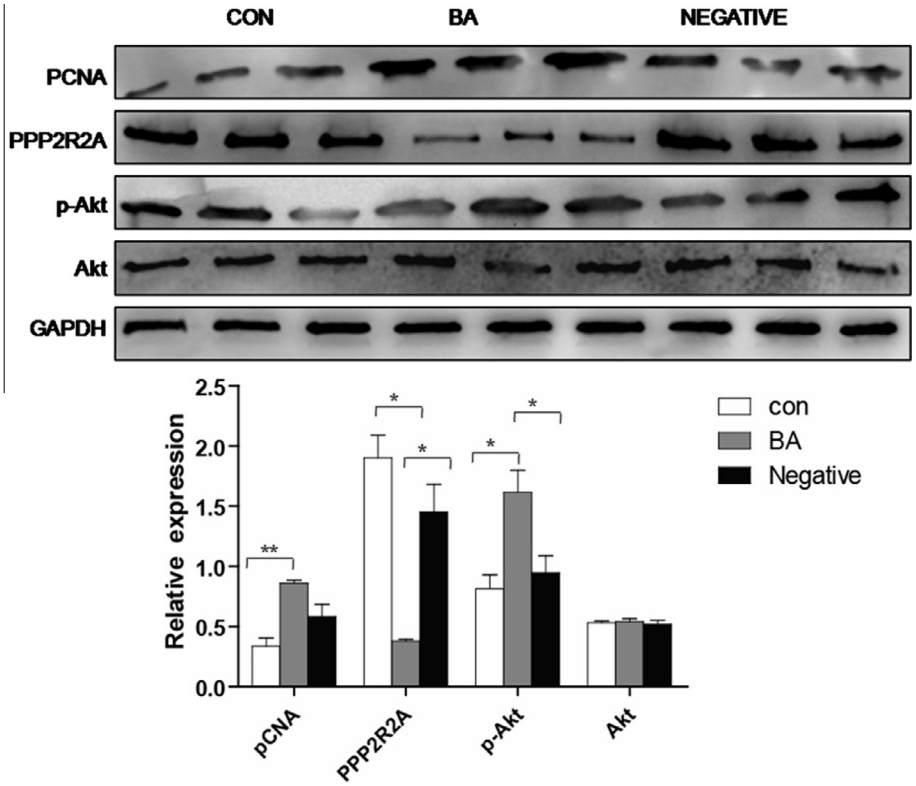

Fig. 3. Three liver samples were randomly chosen from each group for Western blotting. Western blot analysis shows clear differences among the three groups. PPP2R2A has lower expression in the BA group compared to the other similar groups ($p < 0.05$). p-Akt displays the opposite pattern with higher expression in the BA group compared to the other groups ($p < 0.05$). There was no difference in the total Akt among all the three groups. The PCNA protein level was significantly increased in the BA group compared to the control group ($p < 0.05$), while there is no difference between the BA group and the negative group. ($^{*}p < 0.05$, $^{**}p < 0.01$).

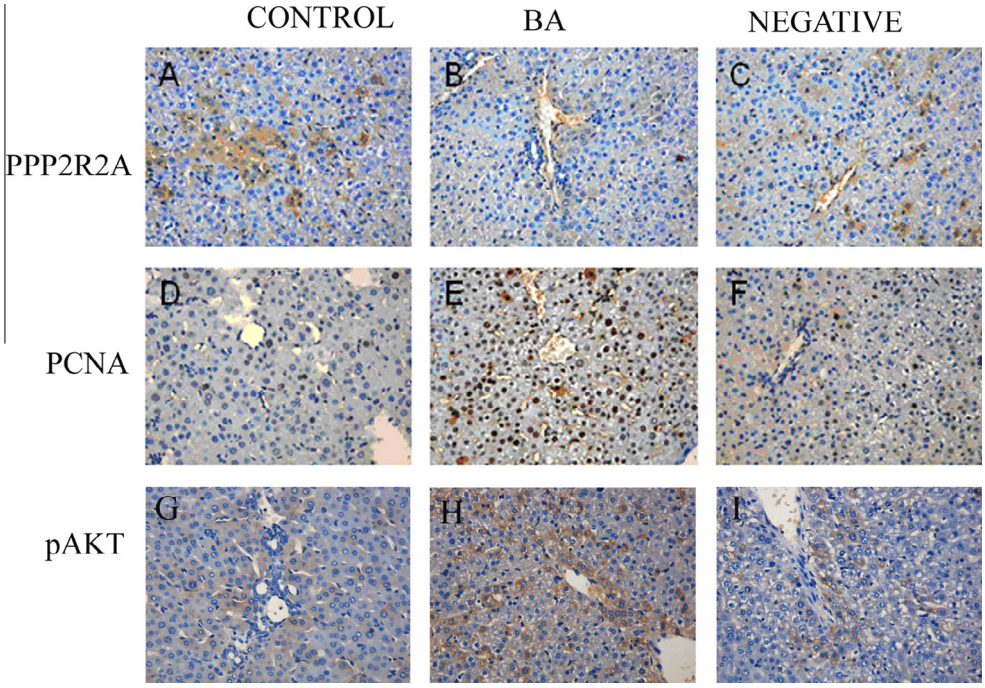

Fig. 4. Representative immunohistochemical staining of PPP2R2A (A–C) and PCNA (D–F). PPP2R2A is expressed in the cytoplasm of liver cells. The control group (A) had a larger positive area with relatively higher intensity compared with the BA group (B) and the negative group (C). For PCNA staining, the BA group (E) had the highest positive rate, while the control group (D) and the negative group (F) had moderately lower levels. (H&E, original magnification × 200).

manner in both human livers and mouse liver fibrosis models [6]. The Akt signaling pathway has been shown to be regulated by miR-222 [7]. Wong and colleagues demonstrated that expression of PPP2R2A 3′untranslated region (UTR) in Hep3B cells was characterized by inhibition of luciferase activity through a miR-222-depdendent mechanism [7]. PPP2R2A protein expression levels were

negatively regulated by miR-222 [7]. PPP2R2A is a regulatory subunit of PP2A, which is essential in the control of Akt activity, and it forms a regulatory link between miR-222 and the Akt signaling pathway [10]. As miRNAs and their biogenesis pathways are highly evolutionarily conserved, our research's aim was to evaluate miR-222's effect on fibrosis in a BA murine model.

In our study, miR-222 was significantly elevated in the BA group when compared with the control and negative groups. Increased miR-222 expression levels were observed in the BA model, which was similar to the expression levels observed in other liver fibrosis models [6]. Through its action on the 3′UTR, miR-222 caused a posttranscriptional decrease in PPP2R2A expression. While the PPP2R2A mRNA level was higher in the control group compared to the negative group, the PPP2R2A protein levels were similar between both groups because of the post transcriptional regulation. Elevated miR-222 expression levels resulted in lower expression levels of PP2R2A resulting in activation of the Akt pathway. The total Akt levels were equal among the three groups. However, the Akt pathway activity, as measured by the level of p-Akt, was higher in the BA group than in the other two groups.

The Akt/PKB pathway plays a central role in regulating signaling of growth factors, cytokines and other cellular stimuli and functions to inhibit apoptosis. Akt phosphorylates and inactivates Bad preventing the release of mitochondrial cytochrome-c and active caspase-9 [14,15]. Research has shown that the Akt signaling pathway inhibited apoptosis in HSC [16] and stimulated HSC proliferation [17]. Our findings indicate that increasing miR-222 levels results in the activation of the Akt pathway and the subsequent activation of HSCs, which play an important role in liver fibrosis.

PCNA is involved in a wide range of cellular functions including DNA replication, repair and epigenetic maintenance [18]. It is often used as a diagnostic marker for cells in S phase cells and undergoing DNA synthesis. Bravo et al. showed that PCNA is a stable protein, which could be detected in quiescent cells for at least 24–48 h after the cells have stopped dividing [19]. The fibrotic liver contained cells that had undergone regeneration. We observed highest mRNA and protein levels of PCNA in the BA group. The ductular proliferation and lobule regeneration seen in H&E sections were consistent with activation of the Akt pathway.

In the current study, we present the finding that miR-222 is overexpressed in mice with BA. The targeting of the 3′UTR of PPP2R2A mRNA by miR-222 resulted in inhibition of PPP2R2A expression levels which consequently led to the loss of dephosphorylation and increased Akt activation. Increasing mir-222 levels as well as upregulation of the downstream Akt pathway profoundly modulated the process of fibrosis, which might represent a potential target for improving BA prognosis.

Conflict of interest

The authors who have taken part in this study declared that they do not have anything to disclose regarding funding or conflict of interest with respect to this paper.

Acknowledgments

This study received financial support from the National Natural Science Foundation of China (Nos. 30973139, 81370472 and 81300517), and The Science Foundation of Shanghai (Nos. 11JC1401300, and 13ZR1451800).

References

[1] J. Hartley, A. Harnden, D. Kelly, Biliary atresia, BMJ 340 (2010) c2383.
[2] M.P. Pakarinen, R.J. Rintala, Surgery of biliary atresia, Scand. J. Surg. 100 (2011) 49–53.
[3] A.B. Haafiz, Liver fibrosis in biliary atresia, Expert Rev. Gastroenterol. Hepatol. 4 (2010) 335–343.
[4] D. Sayed, M. Abdellatif, microRNAs in development and disease, Physiol. Rev. 91 (2011) 827–887.
[5] X.W. Wang, N.H. Heegaard, H. Orum, microRNAs in liver disease, Gastroenterology 142 (2012) 1431–1443.
[6] T. Ogawa, M. Enomoto, H. Fujii, Y. Sekiya, K. Yoshizato, K. Ikeda, N. Kawada, microRNA-221/222 upregulation indicates the activation of stellate cells and the progression of liver fibrosis, Gut 61 (2012) 1600–1609.
[7] Q.W. Wong, A.K. Ching, A.W. Chan, K.W. Choy, K.F. To, P.B. Lai, N. Wong, MiR-222 overexpression confers cell migratory advantages in hepatocellular carcinoma through enhancing AKT signaling, Clin. Cancer Res. 16 (2010) 867–875.
[8] N. Uyama, Y. Iimuro, N. Kawada, H. Reynaert, K. Suzumura, T. Hirano, N. Kuroda, J. Fujimoto, Fascin, a novel marker of human hepatic stellate cells, may regulate their proliferation, migration, and collagen gene expression through the FAK-PI3K-Akt pathway, Lab. Invest. 92 (2012) 57–71.
[9] M. Hanada, J. Feng, B.A. Hemmings, Structure, regulation and function of PKB/AKT–a major therapeutic target, Biochim. Biophys. Acta 1697 (2004) 3–16.
[10] Y.C. Kuo, K.Y. Huang, C.H. Yang, Y.S. Yang, W.Y. Lee, C.W. Chiang, Regulation of phosphorylation of Thr-308 of Akt, cell proliferation, and survival by the B55alpha regulatory subunit targeting of the protein phosphatase 2A holoenzyme to Akt, J. Biol. Chem. 283 (2008) 1882–1892.
[11] C. Petersen, D. Biermanns, M. Kuske, K. Schakel, L. Meyer-Junghanel, H. Mildenberger, New aspects in a murine model for extrahepatic biliary atresia, J. Pediatr. Surg. 32 (1997) 1190–1195.
[12] C. Roderburg, G.W. Urban, K. Bettermann, M. Vucur, H. Zimmermann, S. Schmidt, J. Janssen, C. Koppe, P. Knolle, M. Castoldi, F. Tacke, C. Trautwein, T. Luedde, Micro-RNA profiling reveals a role for miR-29 in human and murine liver fibrosis, Hepatology 53 (2011) 209–218.
[13] Y. Murakami, H. Toyoda, M. Tanaka, M. Kuroda, Y. Harada, F. Matsuda, A. Tajima, N. Kosaka, T. Ochiya, K. Shimotohno, The progression of liver fibrosis is related with overexpression of the miR-199 and 200 families, PLoS ONE 6 (2011) e16081.
[14] S.R. Datta, A. Katsov, L. Hu, A. Petros, S.W. Fesik, M.B. Yaffe, M.E. Greenberg, 14-3-3 proteins and survival kinases cooperate to inactivate BAD by BH3 domain phosphorylation, Mol. Cell 6 (2000) 41–51.
[15] S.R. Datta, H. Dudek, X. Tao, S. Masters, H. Fu, Y. Gotoh, M.E. Greenberg, Akt phosphorylation of BAD couples survival signals to the cell-intrinsic death machinery, Cell 91 (1997) 231–241.
[16] Y. Wang, X.Y. Jiang, L. Liu, H.Q. Jiang, Phosphatidylinositol 3-kinase/Akt pathway regulates hepatic stellate cell apoptosis, World J. Gastroenterol. 14 (2008) 5186–5191.
[17] F.R. Murphy, R. Issa, X. Zhou, S. Ratnarajah, H. Nagase, M.J. Arthur, C. Benyon, J.P. Iredale, Inhibition of apoptosis of activated hepatic stellate cells by tissue inhibitor of metalloproteinase-1 is mediated via effects on matrix metalloproteinase inhibition: implications for reversibility of liver fibrosis, J. Biol. Chem. 277 (2002) 11069–11076.
[18] W. Strzalka, A. Ziemienowicz, Proliferating cell nuclear antigen (PCNA): a key factor in DNA replication and cell cycle regulation, Ann. Bot. 107 (2011) 1127–1140.
[19] R. Bravo, H. Macdonald-Bravo, Existence of two populations of cyclin/proliferating cell nuclear antigen during the cell cycle: association with DNA replication sites, J. Cell Biol. 105 (1987) 1549–1554.